

Ocular aberrations up to the infrared range: from 632.8 to 1070 nm

Enrique J. Fernández and Pablo Artal

Laboratorio de Optica, Universidad de Murcia, Centro de Investigación en Optica y Nanotecnología, Campus de Espinardo, 30071 Murcia, Spain
enriquej@um.es, pablo@um.es

Abstract: Ocular aberrations were measured by using a Hartmann-Shack wavefront sensor in the visible and infrared portions of the spectrum. In the latter, wavelengths 1030, 1050 and 1070 nm were used for the first time for the study of the optical quality of the eye. In this spectral range the retinal photoreceptors barely respond, so the radiation is virtually invisible for the subject. The results were confronted with those obtained by the same system at 780 and 632.8 nm. Monochromatic aberrations were found to be similar from the visible to the infrared. Longitudinal chromatic aberration was experimentally obtained, being approximately 1 D from 632.8 to 1070 nm. The feasibility of using the infrared for studying the eye was demonstrated. The employment of the infrared has an enormous potential for the better understanding of the impact and influence of the aberrations in vision with adaptive optics. It allows for measuring and controlling aberrations whilst the subject might eventually perform visual tests, with no interference from the beacon light.

©2008 Optical Society of America

OCIS codes: (330.5370) Physiological optics; (330.4460) Ophthalmic optics; (010.1080) Adaptive optics.

References and links

1. M. S. Smirnov, "Measurement of the wave aberration of the human eye," *Biophys. J.* **7**, 766–795 (1962).
2. F. Berny and S. Slansky, "Wavefront determination resulting from Foucault test as applied to the human eye and visual instruments," in *Optical Instruments and Techniques*, H. Dickson, 375–386 (Oriel, London, 1970).
3. H. Howland and B. Howland, "A subjective method for the measurement of monochromatic aberrations of the eye," *J. Opt. Soc. Am.* **67**, 1508–1518 (1977).
4. G. Walsh, W. N. Charman, and H. Howland, "Objective technology for the determination of monochromatic aberrations of the human eye," *J. Opt. Soc. Am. A* **1**, 987–992 (1984).
5. D. R. Williams, D. H. Brainard, M. J. McMahon, and R. Navarro, "Double-pass and interferometric measures of the optical quality of the eye," *J. Opt. Soc. Am. A* **11**, 3123–3135 (1994).
6. P. Artal, S. Marcos, R. Navarro, and D. R. Williams, "Odd aberrations and double-pass measurements of retinal image quality," *J. Opt. Soc. Am. A* **12**, 195–201 (1995).
7. I. Iglesias, E. Berrio, and P. Artal, "Estimates of the ocular wave aberration from pairs of double-pass retinal images," *J. Opt. Soc. Am. A* **15**, 2466–2476 (1998).
8. J. Liang, B. Grimm, S. Goelz, and J. F. Bille, "Objective measurement of WA's of the human eye with the use of a Hartmann–Shack wave-front sensor," *J. Opt. Soc. Am. A* **11**, 1949–1957 (1994).
9. J. Liang and D. R. Williams, "Aberrations and retinal image quality of the normal human eye," *J. Opt. Soc. Am. A* **14**, 2873–2883 (1997).
10. P. M. Prieto, F. Vargas-Martín, S. Goelz, and P. Artal, "Analysis of the performance of the Hartmann–Shack sensor in the human eye," *J. Opt. Soc. Am. A* **17**, 1388–1398 (2000).
11. D. R. Griffin, R. Hubbard, and G. Wald, "The Sensitivity of the human eye to infra-red radiation," *J. Opt. Soc. Am.* **37**, 546–553 (1947).
12. P. L. Walraven and H. J. Leebeek, "Foveal sensitivity of the human eye in the near infrared," *J. Opt. Soc. Am.* **53**, 765–766 (1963).
13. D. H. Sliney, R. T. Wangemann, J. K. Franks, and M. L. Wolbarsht, "Visual sensitivity of the eye to infrared laser radiation," *J. Opt. Soc. Am.* **66**, 339–341 (1976).
14. American National Standard Institutes "For the safe use of lasers," ANSI Z136.1-2000, Laser Institute of America, (Orlando, Fla., 2000).

15. F. C. Delori and K. P. Pflibsen, "Spectral reflectance of the human ocular fundus," *Appl. Opt.* **28**, 1061-1077 (1989).
16. Jan van de Kraats, Tos T. J. M. Berendschot, and Dirk van Norren, "The pathways of light measured in fundus reflectometry," *Vision Res.* **36**, 2229-2247 (1996).
17. E. J. Fernández, A. Unterhuber, P. Prieto, B. Hermann, W. Drexler, and P. Artal, "Ocular aberrations as a function of wavelength in the near infrared measured with a femtosecond laser," *Opt. Express* **13**, 400-409 (2005), <http://www.opticsinfobase.org/abstract.cfm?URI=oe-13-2-400>.
18. D. A. Atchison and G. Smith, "Chromatic dispersions of the ocular media of human eyes," *J. Opt. Soc. Am. A* **22**, 29-37 (2005).
19. S. Manzanera, C. Canovas, P. M. Prieto, and P. Artal, "A wavelength tunable wavefront sensor for the human eye," *Opt. Express* **16**, 7748-7755 (2008), <http://www.opticsinfobase.org/abstract.cfm?URI=oe-16-11-7748>.
20. H. Liou and N. A. Brennan, "Anatomically accurate, finite model eye for optical modeling," *J. Opt. Soc. Am. A* **14**, 1684-1695 (1997).
21. R. E. Bedford and G. Wyszecki, "Axial chromatic aberration of the human eye," *J. Opt. Soc. Am.* **47**, 564-565 (1957).
22. W. N. Charman and J. A. Jennings, "Objective measurements of the longitudinal chromatic aberration of the human eye," *Vision Res.* **16**, 999-1005 (1976).
23. P. A. Howarth and A. Bradley, "The longitudinal chromatic aberration of the human eye and its correction," *Vision Res.* **26**, 361-366 (1986).
24. L. N. Thibos, M. Ye, X. Zhang, and A. Bradley, "The chromatic eye: a new reduce-eye model of ocular chromatic aberration in humans," *Appl. Opt.* **31**, 592-599 (1992).
25. E. J. Fernández, I. Iglesias, P. Artal, "Closed-loop adaptive optics in the human eye," *Opt. Lett.* **26**, 746-748 (2001).
26. E. J. Fernández, S. Manzanera, P. Piers, and P. Artal, "Adaptive optics visual simulator," *J. Refract. Surg.* **18**, 634-638 (2002).
27. P. Artal, L. Chen, E. J. Fernández, B. Singer, S. Manzanera, and D. R. Williams, "Neural compensation for the eye's optical aberrations," *J. Vision* **4**, 281-287 (2004).
28. E. J. Fernández and P. Artal, "Study on the effects of monochromatic aberrations in the accommodation response by using adaptive optics," *J. Opt. Soc. Am. A* **22**, 1732-1738 (2005).
29. P. Piers, E. J. Fernández, S. Manzanera, S. Norrby, and P. Artal, "Adaptive optics simulation of intraocular lenses with modified spherical aberration," *Invest. Ophthalmol. Vis. Sci.* **45**, 4601-4610 (2004).
30. L. Chen, P. B. Kruger, H. Hofer, B. Singer, and D. R. Williams, "Accommodation with higher-order monochromatic aberrations corrected with adaptive optics," *J. Opt. Soc. Am. A* **23**, 1-8 (2006).
31. K. M. Hampson, C. Paterson, C. Dainty, and E. A. H. Mallen, "Adaptive optics system for investigation of the effect of the aberration dynamics of the human eye on steady-state accommodation control," *J. Opt. Soc. Am. A* **23**, 1082-1088 (2006).
32. A. Unterhuber, B. Považay, B. Hermann, H. Sattmann, A. Chavez-Pirson, and W. Drexler, "In vivo retinal optical coherence tomography at 1040 nm - enhanced penetration into the choroid," *Opt. Express* **13**, 3252-3258 (2005), <http://www.opticsinfobase.org/abstract.cfm?URI=oe-13-9-3252>.
33. E. C. Lee, J. F. de Boer, M. Mujat, H. Lim, and S. H. Yun, "In vivo optical frequency domain imaging of human retina and choroid," *Opt. Express* **14**, 4403-4411 (2006), <http://www.opticsinfobase.org/abstract.cfm?URI=oe-14-10-4403>.
34. R. Huber, D. C. Adler, V. J. Srinivasan, and J. G. Fujimoto, "Fourier domain mode locking at 1050 nm for ultra-high-speed optical coherence tomography of the human retina at 236,000 axial scans per second," *Opt. Lett.* **32**, 2049-2051 (2007).
35. S. Makita, T. Fabritius, and Y. Yasuno, "Full-range, high-speed, high-resolution 1- μ m spectral-domain optical coherence tomography using BM-scan for volumetric imaging of the human posterior eye," *Opt. Express* **16**, 8406-8420 (2008), <http://www.opticsinfobase.org/abstract.cfm?URI=oe-16-12-8406>.

1. Introduction

In the first stage of vision, optical performance of the eye determines and limits the quality of the images projected onto the retina. From this perspective, the interest for measuring and understanding the optics of the eye is enormous. Since decades, special attention has been paid to objective methods for measuring the ocular aberrations [1-7]. Within the objective methods, the Hartmann-Shack wavefront sensor [8-10] has progressively become the most widely used in the field, possibly due to its relatively simplicity and reliable results when properly implemented. Ocular aberrations have preferably studied under visible light. The rationale is evident provided that visual perception in humans occurs in this spectral range. Nevertheless, the use of near infrared (NIR) is common since some years. A number of factors justify the employment of this spectral range to explore the human eye. Firstly, the retinal

response is weak in the NIR, making illumination more comfortable for the subjects [11-13]. In addition, safety limits for retinal exposure to light are higher in NIR, where solely thermal injury could potentially occur [14]. Another factor is the reflectivity of the retina, which increases with wavelength [15,16]. In this context, systematic characterization of the ocular optics was recently accomplished in the NIR range, from 700 to 900 nm [17]. In the mentioned work, ocular monochromatic aberrations were found to be practically constant in the whole spectral segment, and similar to those found in the visible. That result is of practical importance, since allows for using NIR, while still estimating the optical quality of the eye in the visible. Longitudinal chromatic aberration, or chromatic refraction, was also obtained, being in the order of 0.5 D for the NIR spectral band. This chromatic offset must be taken into account when using such wavelengths for retrieving the aberrations in the visible. Knowing the chromatic aberration in the NIR has allowed for better modeling the optics of the eye in the visible [18]. In the current work, we extended the spectral range for studying the ocular optics, targeting the infrared (IR) beyond 900 nm. Using longer wavelengths might eventually make the beacon light invisible for the observer [11], with potential applications for a number of experiments. Among others, it might become possible to obtain, and eventually control, aberrations by using adaptive optics, so that subjects would not aware of the measuring light. It should permit, for instance, studying vision at low illumination levels, under scotopic and mesopic conditions. In the present manuscript we have studied the feasibility of employing wavelengths up to 1070 nm with standard, silicon-based, detectors coupled in a Hartmann-Shack wavefront sensor. Ocular optics from normal eyes obtained at IR has been characterized and compared with that at visible wavelengths. Advantages and practical applications of using this spectral portion of the spectrum for studying the eye have been also discussed.

2. Methods

The experimental apparatus for measuring ocular aberrations was essentially compounded by a Hartmann-Shack wavefront sensor, three different light sources and appropriate optics for conjugating the eye's exit pupil onto the sensor. It is conceptually similar to a wavelength tunable wavefront sensor for the eye, recently used for the visible part of the spectrum [19]. Figure 1 depicts the set-up showing the main components. The wavefront sensor was formed by a CCD camera (Hamamatsu C5999, Japan) placed at the focal length of an array of microlenses. The camera's CCD chip was based on Silicon with sensitivity typically up to the 1300 nm according to the manufacturer, and enhanced quantum efficiency in the NIR (peak at 800 nm). The camera video format was RS-170 at 30 Hz frame rate, with internal electronic exposure time of 1/500 s. The microlenses were square cells of 0.3 mm and 6 mm focal length. They were implemented in the mount of the camera for simplicity. A telescope formed by two positive achromatic doublets, L1 and L2 of 250 and 150 mm of focal length (-0.6 total magnification), conjugated the eye's exit pupil with the array of microlenses. Lenses had broad antireflection coating, reducing losses in the visible and IR part of spectrum.

The illumination of the eye was accomplished by combining a He-Ne laser, emitting at 632.8 nm; a diode laser, emitting at 780 nm; and an Amplified Spontaneous Emission (ASE) light source for covering the IR portion of the spectrum (Broadband ASE Source – 1 micron band, Multiwave Photonics, Portugal). The latter delivered IR light from a diode pumped Yb-doped fiber, with high spectral density output in the wavelength range of 1025 to 1075 nm. Three interference filters of 10 nm width centered at 1030, 1050 and 1070 nm were placed in front of the ASE source for selecting each wavelength during the runs. Lights of 632.8 and 780 nm were employed in the experiment as references. By using a set of flipping mirrors implemented in the system, the experimenter could easily select the appropriate wavelength during the measurements. Due to the distinct intensity of the light sources, the irradiance reaching the eye had to be adjusted for each wavelength. The system incorporated a scaled continuous neutral filter wheel. Previous calibration allowed for fast regulation of the intensity for each wavelength. Due to the inter-subject variability in fundus reflectance, light irradiance was set for each eye until Hartmann-Shack images were acceptable for retrieving the

wavefront. In all cases, it was kept below 20 μW . The value is more than one order of magnitude below recommended maximum light exposure, according to safety standards [14]. This allowed continuous viewing of the beam with no danger of retinal damage. Ocular aberrations were measured in all the eyes for a pupil of 5.8 mm of diameter.

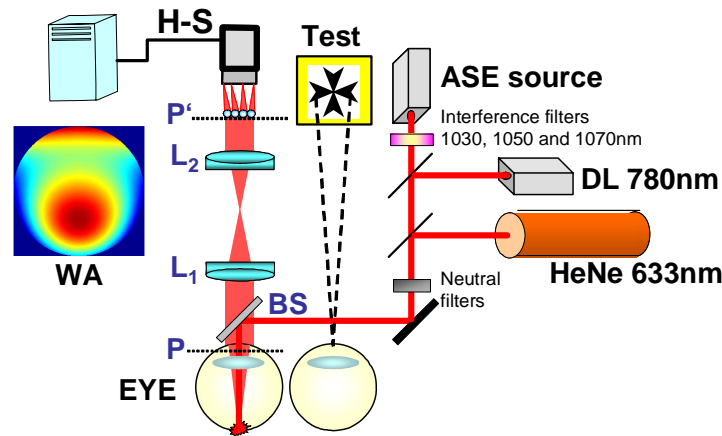


Fig. 1. Experimental set-up. Three light sources illuminated consecutively the eye. Ocular aberrations were obtained by a Hartmann-Shack (H-S) wavefront sensor at wavelengths 632.8, 780, 1030, 1050 and 1070 nm. Fixation test was employed in the system during the runs.

Seven young adults participated in this study with ages ranging from 27 to 37 years old (mean 33.14 and standard deviation 3.24). Refractions ranged from - 4 to + 0.5 D. The system was endowed by a fixation relay, where a back illuminated maltese cross was displayed. This was an important part of the set-up since the IR radiation was invisible, accounting for its low irradiance. Consequently, the beacon light provided no reference for keeping the line of sight and additional stimulus was required. Prior the runs, subjects were asked to subjectively place the stimulus at their remote point, once their pupils were dilated and accommodation paralyzed by instilling two drops of tropicamide 0.5 %. Left or right eye was measured according to the individual preference of each subject, changing the location of the fixation test accordingly. Subjects were aligned to the system by using their personal dental molds, reducing head movements that might affect the measurements. They were allowed to rest and leave the dental impression between runs. For each wavelength, ocular aberrations were estimated as the average aberrations from 128 Hartmann-Shack images. These images were obtained in 4 different runs of 2 s each. All subjects were familiar with the experiment, providing consent for the purpose of the measurements.

Due to the large spectral range employed in the experiment, almost 440 nm, chromatic aberration of the system was first calculated. That was of practical interest, especially for the possible estimation of the eye's chromatic refraction. In order to obtain the chromatic aberration of the apparatus, the system was modeled by using the optical design program Zemax (Zemax Development Corporation, USA). The maximum chromatic aberration was found to occur from 780 to 1070 nm, with a value of 0.025 D. The rest of monochromatic aberrations in the system were negligible, being diffraction limited.

3. Results

The properties of the retina for diffusing or backscatter light in the portion of the spectrum around 1050 nm have not been characterized yet. The longest wavelength considered so far in vivo was 805 nm [15]. Previous works have shown that, in general, scattering increases with wavelength. Figure 2 shows Hartmann-Shack images from several subjects at wavelengths 632.8 and 1050 nm for comparison. In spite of individual differences, Fig. 2 qualitatively

presents a clear increase of scattering for longer wavelengths. In most cases, at 1050 nm diffused light completely filled the space existing across the spots. In some subjects, AB and SM, images corresponding with 632.8 nm exhibited certain amount of scattering. Still, even in those subjects the increase of light diffused at 1050 was evident. In the rest of subjects the boost of scattering was even more dramatic. In most of the cases, the contour of the pupil could be clearly resolved, which might eventually benefit those algorithms for automatic pupil tracking from Hartmann-Shack images.

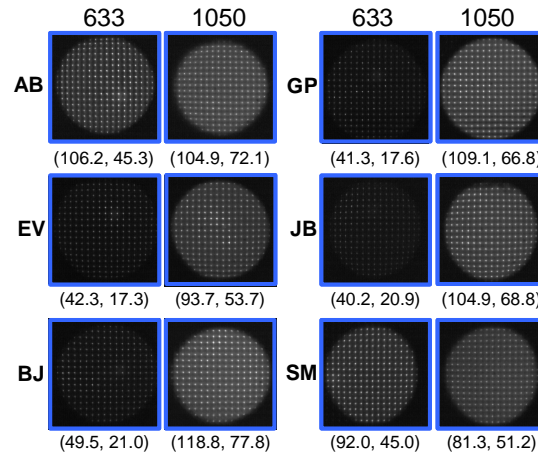


Fig. 2. H-S images obtained from different subjects at 632.8 and 1050 nm showing the augment of scattering with wavelength. Below images, average peak and pedestal value are presented.

Due to the different spectral response of the detector and the distinct irradiance applied for each wavelength, the images presented in Fig. 2 provided solely a qualitatively comparison of the existing change of scattering across wavelengths. In order to obtain numerical estimation, further analysis of the images was performed. For doing so, a systematic procedure was adopted, described in the following.

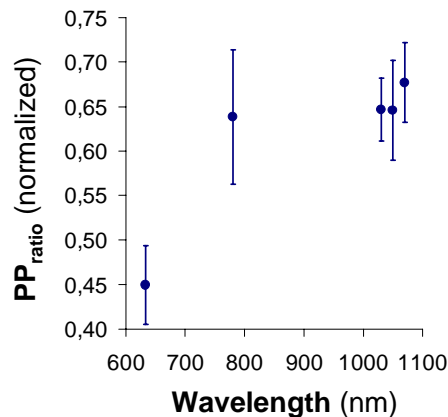


Fig. 3. Average pedestal-peak ratio (PP_R) from all subjects as a function of wavelength. Error bars corresponded to the standard deviation.

Hartmann-Shack images obtained at every wavelength were averaged. The central lines of spots from these images were taken. Corresponding sub-images from the latter, saved with equal width than the squared microlenses, were then processed. Average intensity values from columns were obtained. These data allowed for clearly identifying the spots and the space

across them. Maxima from the spots peaks and average values from the baseline, i.e. inter-spots space, were manually retrieved, and analyzed with the help of some routines written in Matlab (Matlab 7.6, The MathWorks, USA). Averaging was performed in order to obtain two single values from each Hartmann-Shack image: the average peak value and the pedestal or baseline average value. As an estimator of the relative scattering we defined the pedestal-peak ratio (PP_R , the quotient between these two averaged parameters). The PP_R provided a simplified method to numerically compare the degree of scattering from the Hartmann-Shack images. The procedure was systematically applied to all subjects and wavelengths. The results were presented in Figure 3. The PP_R from all subjects is depicted as a function of wavelength. The error bars represent the standard deviation from all subjects. Fig.3 shows a clear jump in the PP_R from 632.8 to 780 nm, indicating a significant change in the scattering. The scattering estimated at 1030, 1050 and 1070 nm was found to be very similar to that at 780 nm. These results could be of importance for modeling the reflectance and diffusion of the retina. The use of light with wavelengths longer than 780 nm for retinal illumination does not seem to produce a significant increase in the scattering.

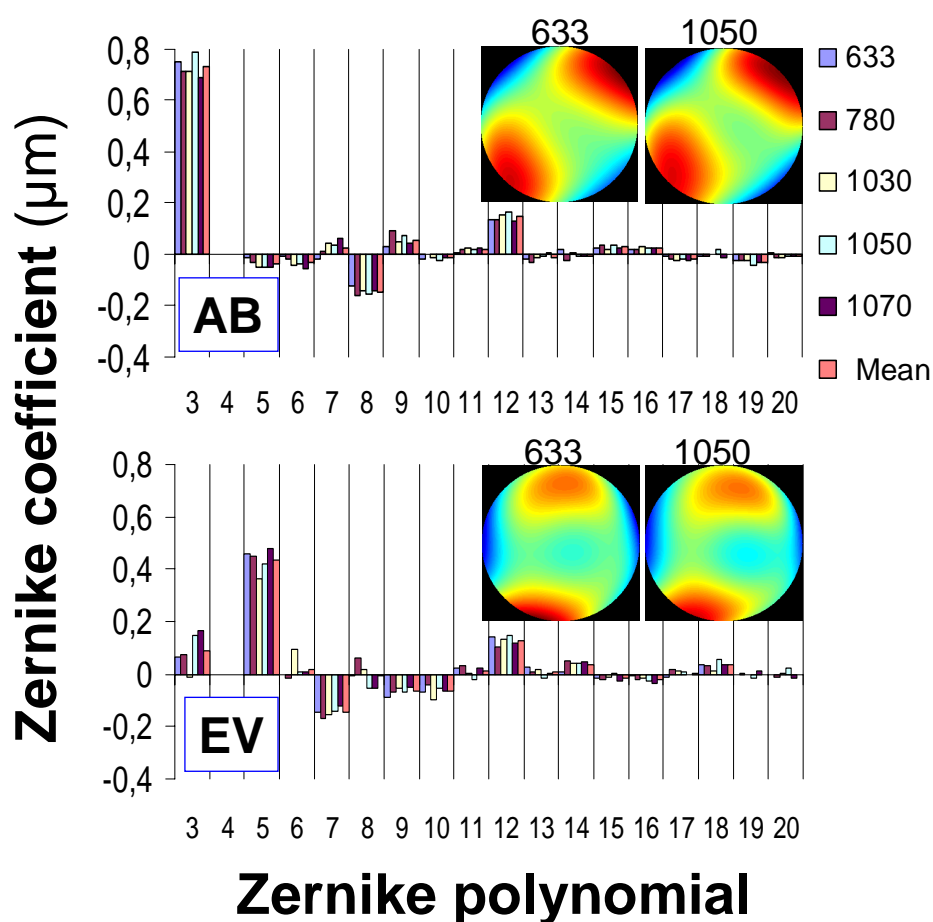


Fig. 4. Zernike coefficients from two subjects at 632.8, 780, 1030, 1050 and 1070 nm, together with aberration maps. The mean value from all wavelengths was also included (pink color).

In a subsequent step, we investigated how monochromatic ocular aberrations in the IR were related with those measured with visible and NIR wavelengths. For each subject ocular aberrations were obtained at every wavelength for comparison. Abrupt changes in the

refractive index of any of the ocular media in the IR would prevent for obtaining similar aberrations in the latter, as compared with those in the visible. Refractive indexes of the ocular media are often taken, when no high accuracy is required, as similar to water. In principle, the refractive index of water does not present a large change in the IR, so from this perspective there is no reason to expect significant variation of the ocular aberrations. Nevertheless, a number of other factors might also affect the measured aberrations. For instance, the crystalline lens is known to present a much complex structure in its refractive index, and perhaps more important, the reflectance of the retina might be quite different in the IR than in the visible. Figure 4 shows the results of measuring monochromatic aberrations in two subjects across all wavelengths with a bars plot. Each color corresponded to a given wavelength. Defocus, represented as the fourth polynomial of Zernike (OSA standard), was not included in the plot and it was studied separately. In Fig. 4 appeared small changes in the Zernike coefficients with wavelength. However, those were small, in the order of magnitude of the variation expected by the Hartmann-Shack wavefront sensor itself. The mean value for each Zernike polynomial was also included in the figure. In Fig. 4 a color coded aberrations maps from these two subjects at the wavelengths 632.8 and 1050 nm was added. The maps showed the good agreement of ocular aberrations across different wavelengths.

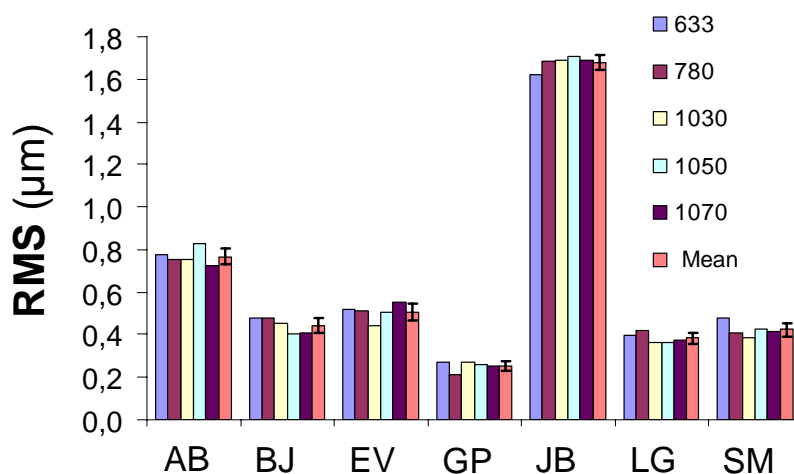


Fig. 5. RMS, excluding defocus, of ocular aberration from each subject for a 5.8 mm pupil size at different wavelengths. Average RMS was shown in pink color. Error bars corresponded with standard deviation.

An alternative way to evaluate the change of aberrations with wavelength, using a single parameter, is calculating the root mean square (RMS) of the wavefront. Figure 5 shows the RMS from all subjects and wavelengths. The mean value was also included. The latter incorporated an error bar which corresponded to the standard deviation. The error bars were similar across subjects. From the figure, it could be also noticed the lack of any trend in the variations of the RMS with wavelength. The term corresponding to defocus was not included in the calculation of the RMS. Once the results concerning monochromatic aberrations have been shown, longitudinal chromatic aberration will be studied in the following.

The longitudinal chromatic aberration was estimated as the difference of defocus obtained from the wavefront sensor for each wavelength. The results from all subjects are presented in Fig. 6, where defocus is shown in diopters. Since the subjects presented different refractions was necessary to adopt a reference for comparing the chromatic defocus. The shortest wavelength 632.8 was taken as the origin for defocus. The experimental results were depicted with black points. The errors bars corresponded to the standard deviation obtained from each subject. As expected, there was a change in defocus connected with the variation of refractive index of the different ocular media. In order to better understand the impact of longitudinal

chromatic aberration in the IR, the figure incorporated the theoretical curve of chromatic defocus, in blue color, proposed by Atchison and Smith 2005 [18]. The curve was also forced for taking 632.8 nm as origin. In the aforementioned reference, the authors compiled a vast set of published experimental measurements of chromatic defocus for finding the best theoretical fit to the data. The spectral range employed was from 400 up to 900 nm. The mathematical function selected for modeling the data was the Cauchy equation. The figure shows that points corresponding with 1030, 1050 and 1070 nm are located away from the theoretical curve. In particular, the distance between the curve and the point corresponding with 1050 nm was 0.15 D. Assuming the parameters of the Cauchy equation are still valid in the IR, a possible explanation for the origin of this effect might be the different penetration of the beam at these wavelengths as compared with that in the visible. For visible light it is usually accepted that most of the light recorded at the wavefront sensor, backscattered from the fundus, originates at the retinal pigment epithelium. Likely, and due to the difference of refractive indexes, the diffusion of light could occur in the border between retinal pigment epithelium and outer segments of photoreceptors. Employing longer wavelengths might allow for deeper penetration into the retinal pigment epithelium. Consequently, light backscattering might happen more efficiently at deeper layers, even though the beam was slightly defocused.

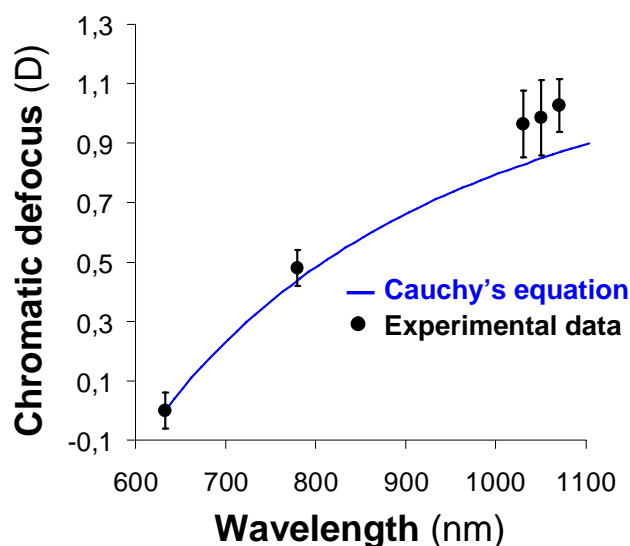


Fig. 6. Averaged chromatic defocus from all subjects as a function of wavelength. Error bars showed the standard deviation.

We theoretically estimated the magnitude of the 0.15 D mismatch. The penetration into the retinal tissue required for placing the experimental point 1050 nm over the theoretical curve was calculated. By using the Liou and Brennan eye model [20], the 0.15 D corresponded to an absolute displacement on the image plane, i.e. the retina, of 0.55 μm .

4. Conclusions

In this work we have demonstrated the feasibility for measuring ocular aberrations in the IR, at 1030, 1050 and 1070 nm, with a standard CCD camera coupled in a Hartmann-Shack wavefront sensor. The camera used in the experiment had a regular Silicon-based CCD detector, making the apparatus cost effective. Other cameras operating in the IR with enhanced performance are commercially available. Specifically, CCD cameras with detectors based on InGaAs offer higher sensitivity in the IR. However, their cost is at least one order of magnitude superior to regular Silicon CCD. For research purposes they might offer

advantages as improved signal-to-noise ratio. Nevertheless, we have demonstrated that standard Silicon CCD still offers enough sensitivity, allowing a significant reduction of the total cost of the experimental set-up. This fact might have a positive impact in the potential use of this new spectral range in clinical applications. In addition, the cost of the system could be further reduced if super luminescent diode laser is employed as light source.

From the analysis of the Hartmann-Shack images it was found that light scattering at 1050 nm was similar to that measured at 780 nm. That indicated that the signal-to-noise ratio appeared comparable, so there were no particular constraints or need for refinement in the Hartmann-Shack algorithms for locating the centroids from the images of the sensor. The use of IR produces in general a similar estimation of the wavefront as compared with that in the visible from the point of view of stability of the measurements. The variance of the RMS, obtained from the variance of the individual Zernike coefficients, shows similar values across wavelengths. As an example showing the typical trend found in the measurements, the error for the RMS from subject AB for wavelength 632.8, 780, 1030, 1050 and 1070 nm was 0.09, 0.13, 0.10, 0.08 and 0.09, respectively. Regarding the PP_R , it should be noted that solely changing the wavelength should produce a slight variation in the aforementioned parameter. The cause could be understood in terms of the broadening of the point spread function caused by increasing the wavelength. In the experiment presented in this work, irradiance was not kept constant, so practical evaluation of the effect was not possible. Moreover, even under such ideal conditions, retina would not backscatter light from different wavelengths with equal efficiency to the sensor. We think the possible effect of broadening the Hartmann-Shack spots associated to wavelength is modest and would not change significantly the trend exhibited in Fig 3.

The chromatic difference of focus was near 1 D from 632.8 to 1070 nm. That was a modest difference as compared to that expected for the same spectral width in the visible. In the latter, a displacement from 400 to 800 nm will generate a chromatic defocus of approximately 3 D [18,21-24]. The parameters of the Cauchy equation proposed by Atchison and Smith [18] for describing chromatic aberration were obtained with experimental data up to 900 nm. Consequently, the equation did not incorporate the possible changes in refractive index occurring in wavelengths beyond. We have assumed in Fig. 6 that the change in chromatic defocus followed a similar trend, so extrapolation of the Cauchy equation up to 1070 nm was possible. Nevertheless, this fact must be taken carefully until experimental confirmation is reported in the future. Possibly, the discrepancy between theoretical curve and experimental points around 1050 nm arouse as a combination of two factors: the parameters describing Cauchy equation might be slightly different, and there might be also a deeper penetration into the retina. The relative contribution of each of these causes is to be determined with further studies.

A result of practical importance is the constancy of the monochromatic aberrations from the visible range up to the IR. This fact allows for effectively measuring the ocular aberrations with IR light, inferring the optical quality of the eye in the visible. The advantage employing IR is, in addition of safety, the lack of any retinal response at the irradiance levels required for using the wavefront sensor. This could have an impact in a number of experiments. In particular, the use of adaptive optics for studying the role and influence of ocular aberrations [25-31] in different aspects of vision could greatly benefit from this novel concept. So far, appropriate instructions must be given to the subjects participating in such experiments, indicating that the beacon light must be neglected and attention must be focused solely in the visual target. Some subjects find difficulties following such instructions, being even unable for performing the experiment. For these subjects the use of IR is particularly suitable. Moreover, visual experiments under mesopic or scotopic conditions, where the stimuli must be kept a low level of irradiance, including experiments of accommodation, are currently impossible to accomplish with simultaneous ocular aberration measurements. In those experiments, the beacon light is more intensely perceived for the subject than the visual stimulus itself. Employing IR illumination overcomes the problem.

In addition, the results presented in this work might also serve as the basis for combining

adaptive optics for ophthalmoscopy in the IR. Recently, the utility of using wavelengths in the surroundings of 1050 nm have been demonstrated in the context of optical coherence tomography [32-35]. In this ophthalmoscopic modality, retinal images obtained in vivo show a deeper penetration into the choroids region, as compared to those obtained in the visible or NIR. Measuring and correcting ocular aberrations in this spectral range might allow for resolving subtle structures of the retina with important clinical application.

Acknowledgments

The authors thanks Wolfgang Drexler for early discussions on employing IR light in the eye and the subjects participating in the study. This research has been supported by the Spanish Ministry of Science (grant FIS2007-64765) and from “Fundación Seneca”, Región de Murcia, Spain (grant 4524/GERM/06).